Study of Integrated High-Performance Regimes with Impurity Injection in JT-60U Discharges

K. W. Hill,[1] W. Dorland,[2] D. R. Ernst,[3] D. Mikkelsen,[1] G. Rewoldt,[1] S. Higashijima,[4] N. Asakura,[4] H. Shirai,[4] T. Takizuka,[4] S. Konoshima,[4] Y. Kamada,[4] H. Kubo,[4] and Y. Miura[4]

[1] Princeton Plasma Physics Lab., Princeton University, PO Box 451, Princeton, NJ 08543, [2] Institute for Plasma Research, Univ. of Maryland, College Park, MD 20742, [3] Plasma Science and Fusion Center, Massachusetts Institute of Technology,Cambridge, MA, [4] Japan Atomic Energy Research Institute, Naka-machi, Naka-gun, Ibaraki-ken, 311-0193 Japan

E-mail: khill@pppl.gov

Abstract. Injection of argon in ELMy H-mode discharges has enabled extension of these plasmas in JT-60U to high density with good confinement and high radiation loss power fraction. By operation of the outer divertor strike point on the divertor dome, confinement improvement, electron density n_e, and radiation-loss power fractions P_{rad} / P_{heat} close to the ITER requirements have been achieved simultaneously ($HH_{98(y,2)} \sim 1$; $n_e \sim 0.8$ n_{GW}, the Greenwald density limit; and $P_{rad} / P_{heat} \sim 0.8$). Linear microstability analyses show a region of reduced growth rate in the argon-seeded discharge for the ITG/TEM mode near r/a = 0.64; the ETG growth rate is greatly reduced across the entire profile and completely quenched around r/a = 0.5 – 0.7. The reduced growth rates are related to the impurity effects, the deuteron dilution, and the temperature gradients.

1. INTRODUCTION

Achievement of high performance plasmas with high density, and acceptable heat loading of the divertor is critical for fusion reactors. Both the steady state divertor heat load and the transient heat load due to ELMs must be reduced in ELMy H-mode plasmas. D_2 puffing can increase the density and reduce the divertor heat load by increasing the radiated power, but it results in confinement degradation at high density. [1] Injection of argon, however, has enabled extension of these plasmas in JT-60U to high density with good confinement and high radiation loss power fraction. [2] By operation of the outer divertor strike point on the divertor dome, confinement improvement, electron density n_e, and radiation-loss power fractions P_{rad} / P_{heat} close to the ITER requirements have been achieved simultaneously ($HH_{98(y,2)} \sim 1$; $n_e \sim 0.8$ times the Greenwald density limit, n_{GW}; and $P_{rad} / P_{heat} \sim 0.8$). Moreover large ELMs, with concomitant large heat fluxes to the divertor plates, can be suppressed. Under these conditions the fuel purity was ~ 70%. To understand the mechanisms by which impurity seeding leads to improved confinement in ELMy H-mode plasmas, linear microstability analyses have been performed using the GS2 gyrokinetic code, [3] without rotation effects, and the FULL code, [4] with and without rotation effects.

2. EXPERIMENTAL SCENARIO

ELMy H-mode plasmas with I_p = 1.2 MA, B_T = 2.5 – 2.6 T, P_{NBI} = 18 MW, elongation = 1.4, and triangularity δ = 0.3 were studied in JT-60U. Discharge E39532 was a plasma in which the outer divertor strike point was kept on the divertor septum or dome (“dome-top” configuration), and both D_2 and argon gas were puffed into the discharge. This shot, at time 7.35 s, was compared with a non-argon reference shot E36349 at 9.05 s in the standard divertor configuration with only D_2 puffing.

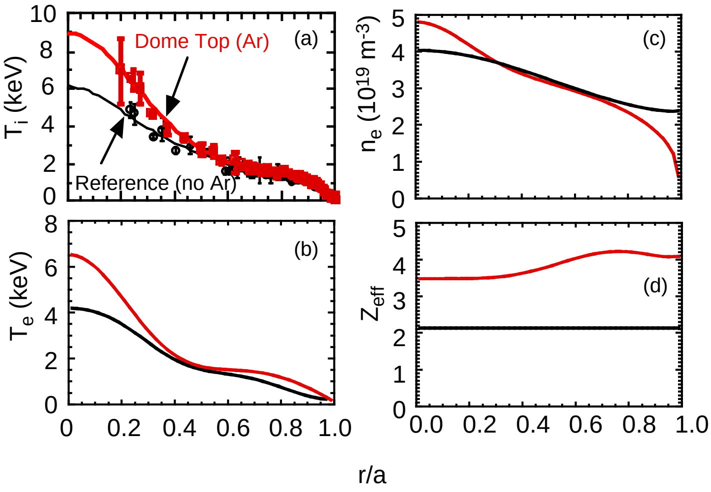

FIG. 1 Radial profiles of T_i, T_e, n_e, and Z_{eff} for argon-seeded, dome-top discharge (red curves) and similar reference shot without argon (black curves).

Both the electron temperature, T_e, and the ion temperature, T_i, are higher in the argon-seeded discharge than in the reference shot, especially in the core, as illustrated in Fig. 1a and 1b. The electron density profile, n_e is somewhat more centrally peaked, and Z_{eff} is higher, due to the argon content. The confinement improvement factors, HH98(y,2), are 0.65 and 1 for the reference and Ar-seeded shots, respectively, the stored energies are 1.9 and 2.5 MJ, and the radiated power fractions are about 50% and 80%. The electron densities are 0.67 times n_{GW} for both shots. The q profiles are monotonic, with positive magnetic shear.

3. MICROSTABILTY ANALYSES

Improved confinement with impurity seeding in other tokamaks has been attributed to reduction of ion thermal transport due to ExB shear suppression of turbulent fluctuations and reduction of toroidal drift wave growth rates [5,6]. Thus, we have performed linear gyrokinetic growth rate calculations without rotation and in the electrostatic limit using the GS2 code [3], for ITG/TEM and ETG modes in the JT-60U discharges, as well as ITG/TEM calculations both with and without rotation effects for the Ar-seeded discharge using the FULL code [4].

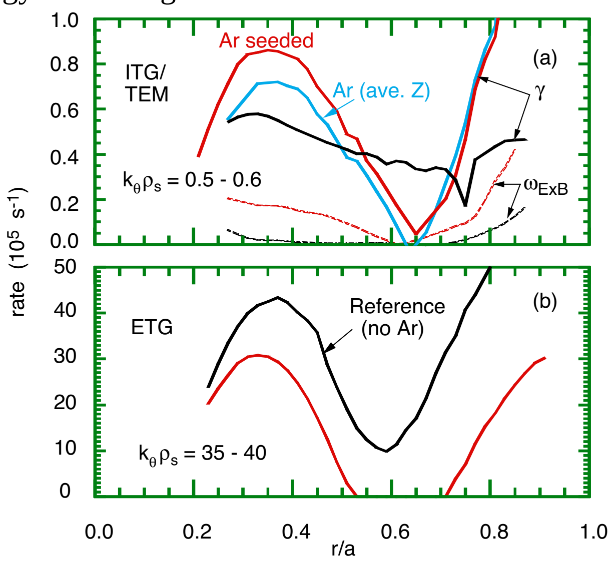

FIG. 2 (1) Maximum linear growth rate, γ and ExB shearing rate of ITG/TEM modes, and (b) γ for ETG mode for argon-seeded discharge (red and blue curves) and non-argon reference shot.

Figure 2 shows that the argon-seeded discharge has a region of significantly reduced linear growth rate for the ITG/TEM mode, γ_{ITG}, near $\rho = r/a = 0.65$, relative to that of the reference shot, and that the ETG mode is also significantly reduced across the entire profile, and is completely quenched over the range $\rho = 0.5 - 0.7$. These rates were calculated with GS2. Here $\rho s = \rho i / \sqrt{2}$, where ρ_i is the ion gyroradius. The reference, non-argon discharge has a significant growth rate for both modes across most of the profile from ρ = 0.2 to ρ = 0.9. Notice that for the unseeded shot (black curves) γ_{ETG} is 25 – 100 times higher than γ_{ITG}. Also note that finite Debye length corrections were inadvertently not included in the ETG calculations; however, inclusion of these effects at ρ = 0.47 and $k_\theta \rho_s$ = 35 resulted in only a 6% decrease in γ_{ETG}, and no change in the real frequency. Near the radii of the minima of the curves in Fig. 2a, the real frequency of the instability changes from positive (ion diamagnetic direction) at smaller radii to negative (electron diamagnetic direction) at larger radii. Thus the plasma transitions from one unstable root to another, going through a minimum in the growth rate. Note that this transition is further out in radius for the non-Ar shot (ρ = 0.75) than for the Ar-seeded shot (ρ = 0.64). In the observed ion temperature profile for the Ar-seeded discharge (Fig. 1a), the slope of the profile shows an increase toward smaller radii which may be related to the minimum in γ_{ITG}. The blue curve in Fig. 2a represents an analysis based on a flat Z_{eff} profile of 3.67. The lower growth rate for the blue curve apparently results from a lower deuteron fraction (about 12% lower) than that for the red curve. The red curve is based on the Z_{eff} profile of Fig. 1d. The shapes of the γ_{ITG} profiles reflect largely the ion temperature gradients, R/L_{Ti}, for the discharges. For the reference discharge R/L_{Ti} is approximately constant, varying only from 11.3 to 12.4 over the large radial range ρ = 0.3 – 0.75, whereas, for the Ar-seeded shot R/L_{Ti} varies widely from a peak value of 18.2 at ρ = 0.4, i.e. near the maximum in the γ_{ITG} profile, to a minimum of 6 at ρ = 0.68, near the minimum in γ_{ITG}.

The effect of rotation on γ_{ITG} as calculated by the FULL code is very small, since the toroidal rotation is small in these high density plasmas with nearly balanced neutral-beam injection. The resulting radial electric field is small, and the ExB shearing rates, ω_{ExB}, [7] are much smaller than γ_{ITG}, as shown by the thin, dashed curves in Fig. 2a. The FULL-code γ_{ITG} profiles for the Ar-seeded discharge both with and without rotation are similar to the red curve in Fig. 2a. With rotation turned on, γ_{ITG} is lower by only about 20% at ρ = 0.6, where γ_{ITG} is already very small, and about 25% at ρ = 0.87. At all other radii the two FULL-code γ_{ITG} curves (with and without rotation) almost overlap.

4. EFFECT OF VARYING IMPURITIES AND TEMPERATURE GRADIENT

The effect on the ITG/TEM growth rate of adding or removing the argon for the two discharges is simulated in Fig. 3. In Fig. 3a the red curve is calculated from a discharge having the T_i, T_e, and n_e profiles of the reference, no-argon shot, with the Z_{eff} and carbon and argon density profiles from the argon-seeded shot. The black curve is the no-argon shot shown in Fig. 2a. The relationship between the red and black growth rate curves is similar to that of the deuteron fraction for the two cases. These fractions for the red and black curves are about 0.64 and 0.68, respectively, at ρ = 0.35, and 0.58 and 0.72 at ρ = 0.7. In Fig. 3b the effect of removing the argon from the argon-seeded discharge (red curve, same as in Fig 1a) is simulated in the black curve. We see that a significantly higher growth rate is predicted near ρ = 0.35, but the growth rate changes little near ρ = 0.65. In this case, the deuteron fraction in the case of the black curve is actually about 0.02 – 0.03 lower than that of the red curve.

The effectiveness of the argon seeding on increasing the critical T_e gradient, R/L_{Tecrit}, for the ETG mode is illustrated in Fig. 4. The linear growth rate is calculated for $k_\theta \rho_s = 35$ at the radial location $\rho = 0.47$ for both the argon-seeded and the reference shots. The critical gradient (R/L_{Te} value at intersection with the horizontal axis) is increased from 2.8 without argon to 4.8 with argon, as indicated by the two left-most arrow heads. The right arrow heads indicate the measured gradients.

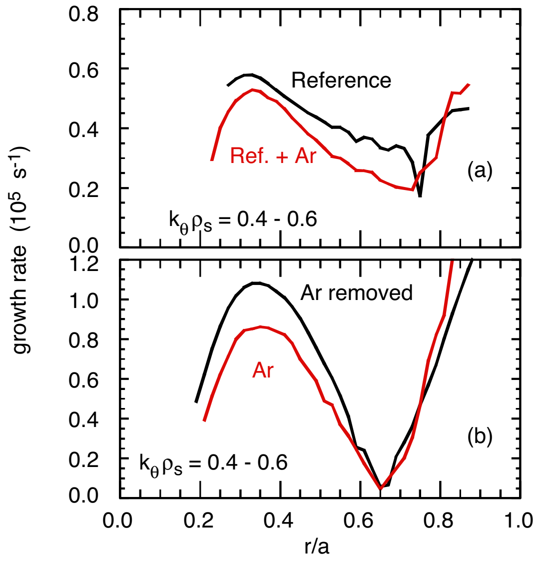

FIG. 3 Simulation of effect on ITG/TEM growth rate of adding argon to non-argon reference shot, and removing the argon from the argon seeded discharge.

5. DISCUSSION

Impurity seeding allows ELMy H-mode plasmas in JT-60U to be extended to higher density while maintaining good confinement. In particular, when combined with high triangularity and dome-top operation, near-ITER requirements of confinement improvement, density, radiated power fraction, and fuel purity can be achieved. The confinement improvement more than offsets the effects of fuel dilution, resulting in increased fusion neutron output. Moreover large ELMs, with concomitant large transient heat fluxes to the divertor plates, can be suppressed. A possible explanation for this suppression, to be investigated, is access to second stability for ideal ballooning modes, as suggested in high-δ discharges without Ar injection. [3] The improved-confinement argon-seeded plasma analyzed in this work showed a significant decrease in the linear growth rate for the ITG/TEM instability near $\rho = 0.65$, a significant reduction of the ETG growth rate across the outer 80% of the plasma, and complete suppression of the ETG in the range $\rho = 0.53 - 0.7$. Simulations in which the deuteron dilution is reduced by about 12% in the Ar-seeded shot by replacing the measured C and Ar by a single, average Z = 10 impurity, result also in a decrease of γ_{ITG} by about 15% across the profile in the region $\rho = 0.25 - 0.6$. Simulations in which the impurities are exchanged between the Ar and reference shots show a large decrease in γ_{ITG} for the reference shot if Ar is added, and a smaller increase in the Ar-seed discharge if the argon is removed. A scan in which R/L_{Te} is varied shows that R/L_{Tecrit} is almost a

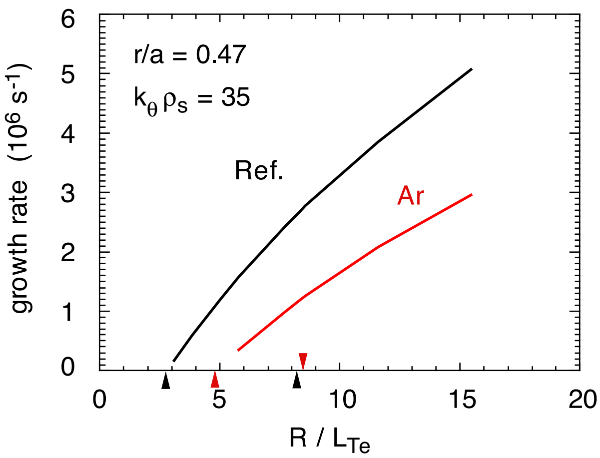

FIG. 4 Growth rate of ETG mode as function of T_e gradient. Arrow heads indicate critical (left) and measured (right) gradients.

factor of 2 higher in the Ar-seeded shot than in the reference shot.

Improved confinement with impurity seeding and ITER-like parameters has been achieved in other tokamaks [5, 6, 8-10] and analysis of the mechanisms for confinement enhancement have been done. [5, 6, 11, 12]. The improved confinement has been correlated with reduced measured turbulence [13], consistent with the model of turbulence causing anomalous transport. In [5] and [6] ExB shearing is reported to be an important mechanism for the improved performance. Although the FULL code analysis indicates that for the JT-60U Ar-seeded discharge ExB shearing has little effect on γ_{ITG} in the high-density, final state, it is still possible that this mechanism is a factor at lower densities, during the evolution to the final, improved-confinement state. The effect of impurities on reducing the ETG growth rate was first studied in [6]. The possibility that ETG turbulence can be relevant to magnetic confinement was reported and analyzed by nonlinear, electromagnetic, gyrokinetic simulations in [14]. For the impurity-seeded, improved-confinement RI mode in TEXTOR, Tokar presented an explanation [12] in which the increased Z_{eff} from impurity seeding reduces the velocity of the ion diamagnetic drift and, thus, the growth rate of the ITG instability. In this case the TEM becomes more important, and leads, through a pinch component of the TEM flux, to density peaking in monotonic-q, positive-shear discharges. The density peaking then leads to further reduction of the ITG instability. Further analysis of the JT-60U argon-seeded and reference discharges needs to be done to quantify the magnitude of increased ExB shearing as a function of time during the evolution of the improved-confinement, discharges, and the radial profiles of the separate ITG, TEM, and ETG instabilities and their relevance to particle and thermal transport.

ACKNOWLEDGEMENTS

Helpful discussions with C. Bourdelle, R. Nazikian, and M. Redi are gratefully acknowledged. The authors wish to thank the members of JAERI who have contributed to the JT-60 project. This work was supported partly by the US Department of Energy under contract no. DE-AC02-76-CH03073.

REFERENCES

[1] N. Asakura *et al.*, Plasma Phys. Control. Fusion **39** (1997) 1295.
[2] H. Kubo *et al*., Phys. Plasmas **9**, (2002) 2127 and Nucl. Fusion **41**, 227 (2001).
[3] M. Kotschenreuther *et al*., Comput. Phys. Commun. **88** (1995) 128.
[4] G. Rewoldt *et al*., Phys. Plasmas **5** (1998) 1815.
[5] M. Murakami *et al*., Nucl. Fusion **41** (2001) 317.
[6] G. M. Staebler *et al.*, Phys. Rev. Lett. **82** (1999) 1692.
[7] T. S. Hahm and K. H. Burrell, Phys. Plasmas **2** (1995) 1648.
[8] J. Ongena *et al.*, Plasma Phys. Control. Fusion **43** (2001) A11.
[9] A. M. Messiaen *et al.*, Nucl. Fusion **34** (1994) 825.
[10] K. W. Hill *et al.*, Phys. Plasmas **6** (1999) 877.
[11] C. Bourdelle *et al*., Nucl. Fusion **42** (2002) 892.
[12] M. Z. Tokar *et al*., Phys. Rev. Lett. **84** (2000) 895.
[13] G. R. McKee *et al*., Phys. Plasmas **7** (2000) 1870.
[14] F. Jenko *et al*., Phys. Plasmas **8** (2001) 4096 and **7** (2000) 1904.